SMALL x, SATURATION, AND DIFFRACTION IN COLLISIONS WITH ELECTRONS, PROTONS AND NUCLEI*

Gösta Gustafson

Department of Astronomy and Theoretical Physics
Lund University, Lund, Sweden
gosta.gustafson@thep.lu.se

The Lund dipole model DIPSY is based on BFKL evolution and saturation. It can be applied to collisions between electrons, protons, and nuclei. In this paper, I present some recent results for exclusive final states in inelastic collisions, a method to generate final states in diffractive excitation, and some results for collisions with nuclei.

1. Introduction

The PYTHIA MC-model is the most successful description of inelastic reactions in DIS and *pp* collisions. It does, however, need input structure functions determined by data, and it also uses simplified assumptions about correlations and diffraction (with parameters retuned at different energies). Our aim is not to obtain the most accurate description, but, instead, to understand underlying dynamics in more detail, also at the cost of lower precision. The results are obtained in collaboration with Christoffer Flensburg and Leif Lönnblad. The outline is the following:

1. Evolution of parton densities to small x.

2. Correlations and fluctuations.

3. Diffraction.

4. Nucleus collisions.

---

* Presented at the International Symposium on Multiparticle Dynamics, Kielce, Poland, September 17–21, 2012.

2. Small x evolution

2.1. Dipole cascade models

Mueller's dipole model

Mueller's dipole cascade model [1] is a formulation of BFKL evolution in transverse coordinate space. Gluon radiation from the color charge in a parent quark or gluon is screened by the accompanying anticharge in the color dipole. This suppresses emissions at large transverse separation, which corresponds to the suppression of small $k_\perp$ in BFKL. For a dipole with transverse coordinates $(\boldsymbol{x}, \boldsymbol{y})$, the probability per unit rapidity (Y) for emission of a gluon at transverse position $\boldsymbol{z}$ is given by

$$\frac{d\mathcal{P}}{dY} = \frac{\bar{\alpha}}{2\pi} d^2\boldsymbol{z} \frac{(\boldsymbol{x} - \boldsymbol{y})^2}{(\boldsymbol{x} - \boldsymbol{z})^2(\boldsymbol{z} - \boldsymbol{y})^2}, \qquad \text{with} \qquad \bar{\alpha} = \frac{3\alpha_{\rm s}}{\pi}. \tag{1}$$

The dipole is split into two dipoles, which (in the large N_c limit) emit new gluons independently. The result is a chain of dipoles, where the number of dipoles grows exponentially with Y.

When two cascades collide, a pair of dipoles with coordinates $(\boldsymbol{x}_i, \boldsymbol{y}_i)$ and $(\boldsymbol{x}_j, \boldsymbol{y}_j)$ can interact via gluon exchange with the probability $2f_{ij}$, where

$$f_{ij} = f\left(\boldsymbol{x}_i, \boldsymbol{y}_i | \boldsymbol{x}_j, \boldsymbol{y}_j\right) = \frac{\alpha_{\rm s}^2}{8} \left[\log\left(\frac{(\boldsymbol{x}_i - \boldsymbol{y}_j)^2(\boldsymbol{y}_i - \boldsymbol{x}_j)^2}{(\boldsymbol{x}_i - \boldsymbol{x}_j)^2(\boldsymbol{y}_i - \boldsymbol{y}_j)^2}\right)\right]^2. \tag{2}$$

Summing over all dipoles in the cascades then reproduces the LL BFKL result.

Lund cascade model DIPSY

The Lund dipole cascade model DIPSY [2, 3] is a generalization of Mueller's model, which includes:

— Important non-leading BFKL effects. The most essential ones are related to energy conservation and the running coupling.

— Saturation from pomeron loops in the evolution. This is not included in Mueller's model or in the BK equation.

— Confinement effects. Needed to satisfy the Froissart bound.

— MC implementation DIPSY. This gives also fluctuations and correlations.

— Applications to collisions between electrons, protons, and nuclei.

At high energies several dipole pairs can interact, and in the eikonal approximation the amplitude is given by

$$T = 1 - e^{-F}, \qquad \text{with} \qquad F = \sum f_{ij}, \tag{3}$$

where the Born amplitude F is given by summing over pairs of a dipole i in the projectile and j in the target. The total and elastic cross sections are then given by $d\sigma_{\text{el}}/d^2b = T^2$, $d\sigma_{\text{tot}}/d^2b = 2T$. Multiple interactions give color loops, which are related to pomeron loops. In the DIPSY model, saturation effects from color loops within the cascade evolution are also included, which makes the result approximately independent of the Lorentz frame used for the analysis.

The DIPSY model and the MC can be applied to collisions with electrons, protons, and nuclei. The coupling of a virtual photon to a $q\bar{q}$ dipole is determined by QED. For a proton, we assume an initial wavefunction represented by three dipoles forming an equilateral triangle. When this is evolved to small x-values, the result is not sensitive to the details of the initial state. For a nucleus, the nucleons are located according to a Wood–Saxon distribution. Results for inclusive and (quasi)elastic observables were presented in Refs. [2–4].

The model can also be used for *exclusive* final states. BFKL describes results for inclusive observables, while the CCFM model [5, 6], and its generalization the LDC model [7, 8], can be used for a description of exclusive states. Some results from Ref. [9] are shown in Fig. 1.
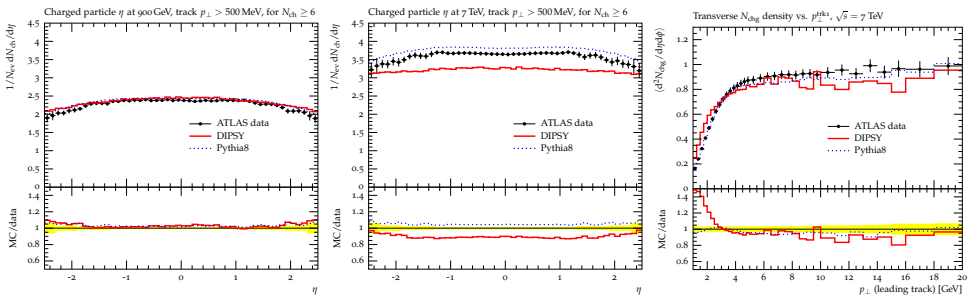

Fig. 1. Minimal bias η distributions at 0.9 and 7 TeV (left and center). Underlying event at 7 TeV: N_{ch} in transverse region *vs* $p_\perp$ for a leading particle (right). Data from ATLAS [10, 11].

3. Correlations and fluctuations

In the MC, it is also possible to calculate *correlations, e.g.* double parton distributions relevant for multiple interactions. We define the double parton

distribution Γ and impact parameter profile F by the relation

$$\Gamma\left(x_1, x_2, b; Q_1^2, Q_2^2\right) \equiv D\left(x_1, Q_1^2\right)\, D\left(x_2, Q_2^2\right)\, F\left(b; x_1, x_2, Q_1^2, Q_2^2\right)\,. \quad (4)$$

Some results from Ref. [12] are shown in Fig. 2, left. We note that for larger Q^2 hotspots develop with increased correlation at small separations b.
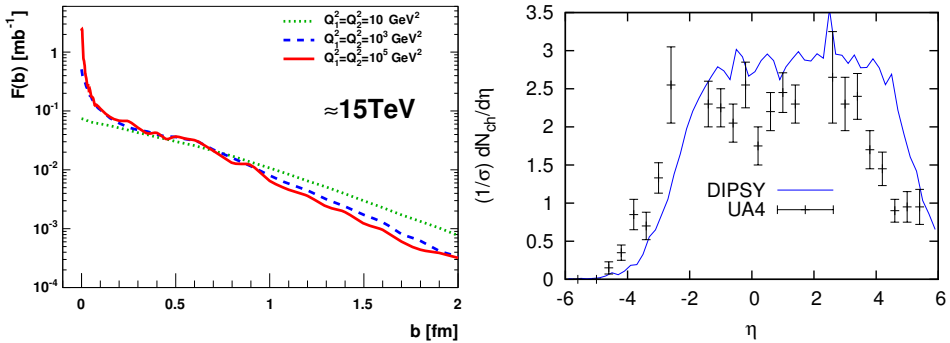

Fig. 2. Left: Two-parton impact parameter profile for proton evolution to $y = 0$ at $\sqrt{s} = 15$ TeV. Right: η-distribution in pp collisions at $\sqrt{s} = 546$ GeV and $\langle M_X \rangle = 140$ GeV, compared to data from UA4 [18].

Fluctuations are very large in QCD evolution. Taking them into account modifies unitarization effects. When the interaction probability fluctuates from event to event, the elastic amplitude is given by $\langle T \rangle = \langle 1 - e^{-F} \rangle$, which is not equal to $1 - e^{-\langle F \rangle}$. This effect suppresses interaction for small b, and enhances it for larger b-values [3]. Fluctuations also give odd eccentricity moments, such as triangular flow in pp and AA collisions (see Refs. [13, 14]).

4. Diffraction

Fluctuations also cause diffractive excitations, as described in the Good–Walker formalism. If the projectile has an internal structure, the mass eigenstates Ψ_k can differ from the eigenstates of diffraction Φ_n, which have different eigenvalues T_n. For an incoming proton the diffractive state is then a different mixture of the mass eigenstates, and the inclusive cross section for diffractive excitation is determined by the variance, $\langle T^2 \rangle - \langle T \rangle^2$, of the amplitude. Assuming that the diffractive eigenstates are represented by parton cascades, some results for cross sections $d\sigma/d\ln(M_X^2)$ in DIS and pp scattering are presented in Ref. [15]. The results do reproduce experimental data from HERA and the Tevatron, and we want to emphasize that the model is tuned only to $\sigma_{\rm tot}$ and $\sigma_{\rm el}$, with no new free parameter.

We also note that for *pp* collisions the fluctuations are very much suppressed for central collisions, when the black limit is approached. Therefore, diffractive excitation is largest for peripheral collisions, in a circular ring expanding slowly to larger radius at higher energy.

Relation Good–Walker *vs* triple-pomeron

Diffractive excitation to high masses is more traditionally described in the triple-regge formalism. In Ref. [16], it is, however, shown that the Good–Walker and triple-pomeron formalisms are just different ways to describe the same phenomenon. Such a relation was also indicated in Ref. [15], where it was demonstrated that the DIPSY results have the expected triple-pomeron form. Switching off the saturation effects in the simulation, the resulting *bare* pomeron corresponds to a single pomeron pole, with an almost constant triple-pomeron coupling. The Good–Walker formalism has then the advantage that the result can be calculated without extra free parameters, also including saturation effects, which in the triple-regge formalism are described by "enhanced diagrams".

Exclusive final states in diffractive excitation

Diffractive excitation is fundamentally a quantum effect. For exclusive final states different contributions interfere destructively, and therefore there is no probabilistic description. Still, it is demonstrated in Ref. [17] how the different contributions can be calculated within the DIPSY MC, added and squared, to give the desired cross section. Some early applications to DIS and *pp* collisions are presented in Ref. [17]. As an example, Fig. 2, right shows the pseudorapidity distribution in *pp* collisions at 546 GeV. We note here that the η-distribution is somewhat too hard for large η. This is due to the lack of quarks in the proton wavefunction, and the resulting absence of a forward baryon. This has to be changed in future improvements. I want to emphasize again that these results are based purely on fundamental QCD dynamics, with no free parameters beyond those tuned to the total and elastic cross sections.

5. Nucleus collisions

The DIPSY model can also be applied to nucleus collisions. Here it gives the full partonic picture, accounting for saturation within the cascades, correlations and fluctuations (it gives *e.g.* triangular flow [14]), and finite size effects. As an example, Fig. 3, left shows the shadowing effect in *p*Pb collisions.

For the final state in nucleus collisions, the model gives a dense gluon soup. This state can be used as initial conditions in a subsequent hydrodynamical expansion. Only adding FSR and hadronization as for hadronic

collisions, would give too many particles, but a toy model, in which the gluons within 1 fm are allowed to interact and reconnect, might simulate the "thermalization" in the final state. As an example, Fig. 3, right shows the resulting multiplicity distribution for $|\eta| < 0.5$ in central collisions at RHIC and LHC.
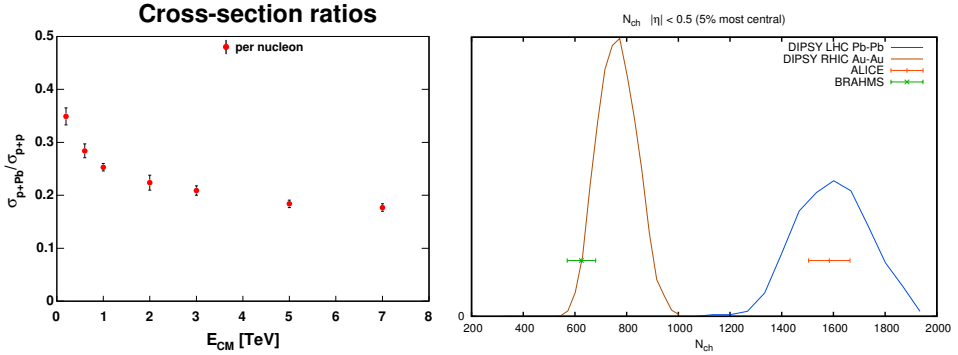

Fig. 3. Left: Shadowing effect $R = \sigma_{pA}/A\sigma_{pp}$ for pPb collisions. Right: Charged multiplicity from toy model "thermalization", in $|\eta| < 0.5$ for central collisions at RHIC (AuAu) and LHC (PbPb).

6. Summary

The DIPSY model is based on QCD dynamics for small x evolution plus saturation. It is an attempt to understand basic dynamics, not to obtain optimal precision.

— It works well for inclusive observables,

— gives a fair description of exclusive final states,

— describes diffraction with no extra free parameter (including exclusive diffractive states),

— includes correlations and fluctuations (goes beyond the meanfield approximation in the BK equation),

— is also applicable to nucleus collisions, where it accounts for saturation within the cascades, correlations, fluctuations, and finite size effects, and can give initial conditions for hydro-expansion.

REFERENCES

[1] A.H. Mueller, *Nucl. Phys.* **B415**, 373 (1994); **B437**, 107 (1995).

[2] E. Avsar, G. Gustafson, L. Lönnblad, *J. High Energy Phys.* **0507**, 062 (2005); **01**, 012 (2007).

[3] C. Flensburg, G. Gustafson, L. Lönnblad, *Eur. Phys. J.* **C60**, 233 (2009).

[4] E. Avsar, G. Gustafson, *J. High Energy Phys.* **0704**, 067 (2007).

[5] S. Catani, F. Fiorani, G. Marchesini, *Nucl. Phys.* **B336**, 18 (1990).

[6] M. Ciafaloni, *Nucl. Phys.* **B296**, 49 (1988).

[7] B. Andersson, G. Gustafson, J. Samuelsson, *Nucl. Phys.* **B467**, 443 (1996).

[8] G. Gustafson, L. Lonnblad, G. Miu, *Phys. Rev.* **D67**, 034020 (2003).

[9] C. Flensburg, G. Gustafson, L. Lönnblad, *J. High Energy Phys.* **1108**, 103 (2011).

[10] G. Aad *et al.* [Atlas Collaboration], *New J. Phys.* **13**, 053033 (2011).

[11] G. Aad *et al.* [Atlas Collaboration], *Eur. Phys. J.* **C71**, 1577 (2011).

[12] C. Flensburg, G. Gustafson, L. Lönnblad, A. Ster, *J. High Energy Phys.* **1106**, 066 (2011).

[13] E. Avsar *et al.*, *J. Phys. G* **38**, 124053 (2011).

[14] C. Flensburg, arXiv:1108.4862 [nucl-th].

[15] C. Flensburg, G. Gustafson, *J. High Energy Phys.* **1010**, 014 (2010).

[16] G. Gustafson, arXiv:1206.1733 [hep-ph], to be published in *Phys. Lett.* **B**.

[17] C. Flensburg, G. Gustafson, L. Lönnblad, arXiv:1210.2407 [hep-ph].

[18] D. Bernard, *et al.* [UA4 Collaboration], *Phys. Lett.* **B166**, 459 (1986).